

## 1 Title Page

## 2 Title

3 Comprehensive profiling of liver x receptor splicing in triple negative breast cancer  
4 reveals existence of novel splice variants that are prognostic for survival

## 5 Authors

6 Priscilia Lianto<sup>1</sup>, J. Bernadette Moore<sup>1</sup>, Thomas A. Hughes<sup>2</sup>, James L. Thorne<sup>1,€</sup>.

7 <sup>1</sup>School of Food Science and Nutrition, University of Leeds, Leeds, LS2 9JT, UK.

8 <sup>2</sup>School of Medicine, University of Leeds, Leeds, LS9 7TF, UK.

9 €Corresponding author

## 10 | Highlights

- 11 • Expression of full length LXR $\alpha$  is associated with shorter disease-free survival of triple  
12 negative breast cancer patients
- 13 • A systematic evaluation of cell lines and primary tumour samples indicates LXR splicing  
14 is extensive in breast cancer
- 15 • Confirmation of three new LXR splice variants at transcript and protein level
- 16 • Expression of full length LXR $\beta$  or LXR $\alpha$  splice variants that harbour truncated ligand  
17 binding domains are associated with better prognosis

- 18       • Expression of LXR target genes is positively correlated with LXR $\alpha$  in relapsed patients  
19           and inversely correlated with LXR $\beta$  in survivors.

## 20 | Abstract

21 | The liver x receptors (LXR) alpha and beta are ligand-responsive transcription factors that link  
22 homeostatic control of lipid metabolism with cancer pathophysiology and prognosis. LXR  
23 activity is elevated in triple negative breast cancer relative to other breast cancer subtypes,  
24 driving gene signatures associated with drug resistance and metastasis. The loci encoding  
25 LXR $\alpha$  and LXR $\beta$  produce multiple alternatively spliced proteins, but the true range of variants  
26 and their relevance to cancer remain poorly defined. Seven splice variants of LXR $\alpha$  or LXR $\beta$   
27 were detected. Three have not been recorded previously and five were prognostic. High  
28 expression of full length LXR $\alpha$  was associated with shorter disease-free survival but splice  
29 variants harbouring truncations of the ligand binding domain were prognostic for improved  
30 survival. All LXR $\beta$  variants were associated with longer disease-free survival. Mechanistically,  
31 while full length LXR $\alpha$  positively correlated with target gene expression in primary samples,  
32 LXR $\beta$  was inversely correlated. We conclude that canonical LXR $\alpha$  function is an oncogenic  
33 driver of triple negative tumour pathophysiology that can be countered by high expression of  
34 truncated splice variants and/or full length LXR $\beta$ .

## 35 | 1. Introduction

36 Breast cancer (BCa) is the most commonly diagnosed cancer in women in the UK and  
37 is the cause of ~600,000 cancer death worldwide [1]. The triple-negative BCa (TNBC)  
38 subtype has higher rates of recurrence in the first three years after prognosis and  
39 increased mortality rates [2]. TNBC is defined by low oestrogen (ER), progesterone  
40 (PR), and Her2 receptor expression. Due to this lack of expression of therapeutic  
41 molecular targets primary disease can only be systemically treated with cytotoxic  
42 chemotherapy and TNBC remains a cancer of unmet clinical need; novel targeted  
43 therapies are urgently needed.

44 Nutritional and epidemiological studies indicate that cholesterol metabolism may play  
45 a role in the aetiology and severity of TNBC [3-6]. The liver x receptors (LXR $\alpha$ /NR1H3;  
46 LXR $\beta$ /NR1H2) are homeostatic regulators of cholesterol metabolism and as such have  
47 been suggested as potential therapeutic targets. LXR $\alpha$  activation by hydroxylated  
48 cholesterol (oxysterols) has been linked to poor survival by driving multi-drug  
49 resistance in TNBC patients [7], and increased metastasis in mouse models [8, 9]. On  
50 the other hand, LXR $\beta$  activation by histamine conjugated oxysterols such as  
51 dendrogenin A can induce lethal autophagy in breast cancer [10]. Intriguingly, ER-  
52 negative and ER-positive BCa subtypes respond differently to LXR ligands [11] even  
53 though oxysterol concentrations are similar between BCa subtypes [12]. Collectively,  
54 these data imply that the differential control over LXR's transcriptional regulation  
55 between subtypes is not simply at the level of ligand type or concentration.

56 LXR $\alpha$  and LXR $\beta$  are each thought to be translated from their own single main  
57 transcript variants, producing 447 and 460 amino acid proteins respectively [13, 14].

58 These ‘full-length’ isoforms harbour domains that provide distinct functions, including  
59 activation function 1 (AF1), hinge region (H), DNA binding domain (DBD) and ligand  
60 binding domain (LBD) [13], as is typical for many ligand dependent nuclear receptors.

61 Aside from the canonical full-length LXR $\alpha$ 1, four additional LXR $\alpha$  splice variants have  
62 been reported in human cell lines or tissue samples to date [15, 16], and a single report  
63 found one alternative splice variant to the major LXR $\beta$ 1 isoform [17]. These studies  
64 found alternative splicing of LXR disrupts the integrity of the DNA and ligand binding  
65 domains, rendering the proteins with reduced or even absent response to ligand [13,  
66 14]. In the case of LXR $\beta$ , a single known splice variant functions as an RNA co-  
67 activator [17]. Genomic and proteomic databases, such as NCBI, TCGA Splicing  
68 Variants database (TSVdb), ENSEMBL, and UNIPROT indicate that both LXR $\alpha$  and  
69 LXR $\beta$  are far more extensively spliced than has been reported. An analysis of splicing  
70 in the nuclear receptor superfamily predicted LXR $\alpha$  has 62 different transcript variants  
71 [18], making it the most extensively spliced nuclear receptor.

72 However, experimental evidence for the existence of such an array of isoforms is  
73 lacking. Given the strong links between cholesterol metabolism, for which the LXRs  
74 play vital regulatory roles, and TNBC aetiology, the aim of this study was to describe  
75 the LXR splice repertoire and clinical significance in human triple negative breast  
76 cancer.

## 77 2. Materials and Methods



## 78 2.1 Systematic transcript variant analysis in public databases

79 The NR1H3/LXR $\alpha$  and NR1H2/LXR $\beta$  spliced variant sequences were assessed in  
80 NCBI and ENSEMBL databases. Sequence annotation records of LXR $\alpha$  and LXR $\beta$   
81 spliced variant read from databases were stored in a feature library created with apE  
82 plasmid editor. This feature library can then be used to scan any nucleotide and/or  
83 amino acid sequence that are complementary to all alternative forms of the LXR $\alpha$   
84 and/or LXR $\beta$  sequences recorded in this library. The number of nucleotides in each  
85 exon and intron were counted in ApE plasmid editor to determine the proportions for  
86 drawing squares and lines represented exons and introns. The schematic diagrams of  
87 LXR variant structures were drawn using AutoCAD (Autodesk, US) software are  
88 shown in **Fig1**, **SF1**, and naming convention used in this study is described in  
89 Supplementary Information Section 1: Isoform naming rationale. Variants are listed in  
90 **TableS1 (LXR $\alpha$ )** and **TableS2 (LXR $\beta$ )**.

## 91 2.2 The Cancer Genome Atlas (TCGA) Splicing Database Analyses

92 TCGA splicing variants database (TSVdb) was searched and LXR splicing expression  
93 data in BCa tumour tissue, reported as normalised RNA-Seq by Expectation  
94 Maximisation (RSEM) values, were downloaded using the TSVdb webtool  
95 (<http://www.tsvdb.com>) [19]. Unreported and/or missing clinical status of the  
96 deposited TCGA BCa tumour samples were replenished by assessing patient tumour  
97 sample information from cBioportal (<http://cBioportal.org>) [20].

## 98 2.3 Human samples: ethical approval, collection, and processing

99 Thirty-eight frozen tumour samples were obtained with ethical approval from the Leeds  
100 Breast Research Tissue Bank (15/HY/0025 and LBTB\_TAC\_1/17). The  
101 clinicopathological features and selection criteria of these cohorts have been  
102 described previously [7, 11, 12, 21] (**Table-S3**). The Leeds TNBC tumour cohorts were  
103 grouped based on their disease-free survival (DFS) status. TNBC patients who did not  
104 have disease relapse during follow-up (median follow-up time was 96 months) were  
105 categorised to 'No Event' group. Meanwhile, TNBC patients who had relapsed and/or  
106 died due to their disease were grouped to an 'Event' group (median follow-up time was  
107 20 months).

## 108 2.4 Cell culture

109 The HEPG2, MCF7, BT474, MDA.MB.231, MDA.MB.468, MDA.MB.453, and  
110 MDA.MB.157 cell lines were originally obtained from ATCC (Manassas, USA). Cell  
111 lines were routinely cultured in Dulbecco's Modified Eagle Medium (DMEM; Thermo  
112 Fisher, UK, Cat. 31966047), supplemented with 10% Fetal Bovine Serum (FBS;  
113 Thermo Fisher, UK, Cat. 11560636) and incubated in 37°C, 5% CO<sub>2</sub>. Cells were  
114 periodically checked and confirmed to be mycoplasma free.

## 115 2.5 siRNA transfection

116 siRNA transfection was performed as previously reported [22]. Briefly,  $1 \times 10^5$  cells  
117 were plated in 6-well plates and incubated overnight. Lipofectamine RNAiMAX  
118 (Thermo Fisher, UK, Cat. 13778030), siLXR $\alpha$  (Origene, USA, Cat. SR322981) and  
119 siLXR $\beta$  (Origene, USA, Cat. SR305039) or the scrambled siRNA (Origene, USA, Cat.

120 SR30004) were diluted in OptiMeM (Thermo Fisher, UK, Cat. 31985062), and added  
121 to the cells at a final concentration of 30 nM. The cells were incubated and after 20 h  
122 the media was removed and fresh DMEM added. Knockdown was confirmed at the  
123 protein level 48 h post-transfection.

## 124 2.6 mRNA extraction, cDNA synthesis, and qPCR

125 Total RNA was isolated from approximately  $5 \times 10^5$  cells using the ReliaPrep™ RNA  
126 Cell Miniprep System (Promega, UK, Cat. Z6012) following product guidelines,  
127 including on column digestion of gDNA. Cytoplasmic RNA was isolated from  
128 approximately  $2 \times 10^6$  cells using the Cytoplasmic & Nuclear RNA Purification Kit  
129 (Norgen, Belmont, CA, USA, Cat. 21000). The concentration of isolated RNA was  
130 determined spectrophotometrically, and RNA purity was evaluated by 260/230 nm and  
131 260/280 nm ratios using a CLARIOstar plate reader (BMG LABTECH, Germany).  
132 cDNA was synthesised from 2 µg RNA using the GoScript™ Reverse Transcription  
133 kit (Promega, UK, Cat. A5003). Primers were designed using NCBI BLAST primer  
134 design or, where transcript variants were not available in the NCBI database, primer  
135 3 software was used [23]. Genomic DNA was digested, and cytoplasmic RNA was  
136 extracted to ensure intron retention was not confused with gDNA or incompletely  
137 spliced transcript. Amplicon size was restricted between 80 to 150 bp and amplicons  
138 were required to span an exon-exon boundary. Primer efficiency was measured from  
139 qPCR standard curves, and primers were redesigned if amplification efficiency did not  
140 fall within 90-110% and/or a single peak was not observed in melting temperature  
141 analysis. A description of primer design strategy is provided in Supplementary

142 Information Section 2: Primer design strategy. Primer positions are shown in **SF2** and  
143 sequences provided in **Table-S4**.

## 144 2.7 Protein lysate extraction

145 Five mg fresh-frozen tumour biopsy samples were homogenised with a 1 mL Dounce  
146 tissue grinder (SLS, UK, Cat. HOM3580). Cell pellets and/or tumour samples were  
147 lysed in RIPA buffer (10 mM Tris-HCl pH 8, 140 mM NaCl, 0.1% SDS, 1% Triton X-  
148 100, 0.1% sodium deoxycholate, 1 mM EDTA, 0.5 mM EGTA), with 1 mM PMSF  
149 (Thermo Fisher, UK, Cat. 78440) added fresh prior to use. The lysed pellets were  
150 incubated on ice for 5 min and centrifuged at 11,500xg at 4°C for 10 min. The protein  
151 lysates concentrations were determined using a BCA kit (Thermo Fisher, UK, Cat.  
152 23227) and lysates were kept in -80°C until further analyses. Each tumour sample was  
153 split in two and duplicate extractions were made. For each protein quantified (see 2.9)  
154 both duplicates were run and the average of each was used for analysis. Concordance  
155 of duplicates was high and is shown in **SF3**.

## 156 2.8 Cytoplasmic and Nuclear Protein Extraction

157 For the cytoplasmic and nuclear protein extractions, the REAP  
158 (Rapid Efficient And Practical) protocol [24] was followed with a slight modification. In  
159 brief,  $1 \times 10^7$  cells were suspended in 1 mL ice cold PBS with 1 mM PMSF. 200  $\mu$ L of  
160 cell lysate was taken, put into a new chilled Eppendorf tube and centrifuged at 1,500  
161 rpm for 3 min at 4°C. Supernatant was removed. The cell pellet (from 200  $\mu$ L cell  
162 lysate) was resuspended in RIPA buffer with 1 mM PMSF (Thermo Fisher, UK, Cat.

163 78440) added fresh prior to use and labelled as a “whole cell fraction”. The remaining  
164 800  $\mu$ L cell lysate was centrifuged at 11,500xg at 4<sup>o</sup>C for 10 s. The supernatant was  
165 removed. The cell pellet (from 800  $\mu$ L cell lysate) was resuspended in 200  $\mu$ L ice-cold  
166 PBS+0.1 NP40 with 1 mM PMSF and centrifuged at 11,500xg at 4<sup>o</sup>C for 10 s. The  
167 supernatant was taken into a new chilled Eppendorf tube and labelled as a  
168 “cytoplasmic fraction”. The cell pellet was then resuspended in 200  $\mu$ L ice-cold  
169 PBS+0.1 NP40 with 1 mM PMSF and centrifuged at 11,500xg at 4<sup>o</sup>C for 10 s. The  
170 supernatant was removed and cell pellet resuspended in 50  $\mu$ L RIPA buffer with 1 mM  
171 PMSF. Cell lysate was sonicated with a water-bath sonicator (Diagenode Bioruptor  
172 Pico, Belgium, Germany) with cycles of 10 s on and 10 s off for five cycles, followed  
173 by centrifugation at 11,500 g at 4<sup>o</sup>C for 10 min. The supernatant was taken, put into a  
174 new chilled Eppendorf tube, and labelled as a “nuclear fraction”. The protein lysates  
175 concentrations were determined using a BCA kit and lysates were kept in -80<sup>o</sup>C until  
176 further analyses.

## 177 2.9 Immunoblotting

178 Forty-five micrograms of protein lysate combined with NUPAGE LDS sample loading  
179 buffer (Thermo Fisher, UK, Cat. NP0007) and DTT reducing agent (Thermo Fisher,  
180 UK, Cat. NP0004) was heated at 70<sup>o</sup>C for 10 min. For LXR variant expression, the  
181 protein lysate was loaded onto a 10% SDS polyacrylamide gel, electrophoresed at  
182 constant 80 V for 150 min, and transferred onto a PVDF membrane (Merck, UK, Cat.  
183 IPFL00010). The membrane was then blocked with TBS Odyssey Blocking Buffer (LI-  
184 COR Biosciences, UK, Cat. 92750000) for 1 h. Proteins were probed with anti-LXR $\alpha$

185 (R&D Systems, USA, Cat. PP-PPZ0412-00, dilution 1/1000), anti-LXR $\beta$  (Active Motif,  
186 Germany, Cat. 61177, dilution 1/1000), and anti-HPRT (Santa Cruz Biotechnology,  
187 Cat. sc-376938, dilution 1/100) overnight at 4°C. The membrane was then blocked  
188 and probed with LICOR secondary antibodies (IRDye 800CW goat anti-mouse Cat.  
189 926-68170, IRDye 680RD goat anti-rabbit Cat. 926-68071; dilution 1/15,000, LI-COR  
190 Biosciences, UK) for 1 h and signal was visualised using the Odyssey system (LI-COR  
191 Biosciences, UK). Densitometry was performed using Image Studio™ Lite (LI-COR  
192 Biosciences, UK) software.

## 193 2.10 Immunoprecipitation

194 One mg protein sample was precleared with Dynabeads Protein A (Thermo Fisher,  
195 UK, Cat.100002D) and 1  $\mu$ g isotype IgG2a (Cell Signalling, USA, Cat. 61656S).  
196 Immunoprecipitation was performed by incubating 40  $\mu$ L of Dynabeads Protein A  
197 coupled to 2  $\mu$ g of anti-IgG2a or 2 $\mu$ g of anti-LXR $\alpha$  using  
198 bis(sulfosuccinimidyl)suberate (Thermo Fisher, UK; Cat. A39266) with 1 mg  
199 protein sample overnight at 4°C. Dynabeads were washed 3 times with 10 mM Tris-  
200 HCl, 50 mM KCl (pH 7.5) and sample eluted in 20  $\mu$ L of NUPAGE LDS sample loading  
201 buffer containing 100 mM DTT, then heated at 70°C for 10 min 10 at 70°C. The  
202 supernatant was transferred to a new Eppendorf tube after being separated from  
203 Dynabeads using a magnetic separator (Promega, UK, Cat. CD4002).

## 204 2.11 In-silico peptide mass prediction

205 The amino acid sequences of LXR variants downloaded from NCBI, ENSEMBL,  
206 and/or UNIPROT databases were subjected to the PeptideMass tool  
207 (<http://www.expasy.org/tools/peptide-mass.html>; Swiss Institute of Bioinformatics,  
208 Switzerland) [25] to theoretically trypsin digest the protein sequence in silico. A set of  
209 peptides from each LXR variant were then subjected to Diagram Venn  
210 (<http://bioinformatics.psb.ugent.be/webtools/Venn>; Bioinformatics & Evolutionary  
211 Genomics, Belgium) in order to find the unique peptides of each LXR variant.

## 212 2.12 S-Trap column coupled Mass Spectrometry (MS)

213 Protein samples were processed using the S-TRAP Micro column (PROTIFI, NY,  
214 USA) following the manufacturer's instructions. Proteins were fully solubilised by  
215 adding 20  $\mu$ L of 10% SDS solution to 20  $\mu$ L sample in RIPA buffer. Reduction  
216 and alkylation were then performed. DTT was added to a final concentration of 20 mM  
217 before heating to 56 °C for 15 min with shaking. The sample was left to cool for 5 min  
218 then iodoacetamide was added to a final concentration of 40 mM, before heating to  
219 20 °C for 15 min with shaking in the dark. Phosphoric acid was then added to a final  
220 concentration of 1.2%, to ensure destruction of all enzymatic activity and  
221 maximise sensitivity to proteolysis. Samples were then diluted with S-Trap binding  
222 buffer (100 mM TEAB pH 7.1 in methanol), and 1 $\mu$ g of trypsin, reconstituted in  
223 50mM triethylammonium bicarbonate (TEAB), was added before the sample was  
224 quickly loaded onto the S-trap column. Proteins were captured within the submicron  
225 pores of the three-dimensional trap. Proteins captured within the trap present  
226 exceptionally high surface area allowing them to be washed free of contaminants. The

227 S-trap was washed by adding 150  $\mu$ L binding buffer before being spun at 4000xg for  
228 30 s. 30  $\mu$ L of 0.02  $\mu$ g/ $\mu$ L Trypsin (Promega, WI, USA) was then added to the top of  
229 the S-trap. S-traps were loosely capped and placed in a 1.5mL Eppendorf and heated  
230 to 46 °C for 15 min with no shaking. Digested peptides were eluted by first spinning  
231 the S-trap at 4,000 g for 1 min. Further elution was performed in 40  $\mu$ L 50mM TEAB,  
232 40  $\mu$ L 0.2% formic acid, and 30  $\mu$ L 50% acetonitrile with 0.2% formic acid prior to  
233 centrifugation. Eluates were combined then dried down prior to resuspension in 0.2%  
234 formic acid.

## 235 2.13 Statistical analyses

236 All statistical analyses were performed using GraphPad Prism v8. The expression of  
237 LXR splice variants in TCGA tumours compared with the adjacent normal tissues was  
238 assessed using a Mann-Whitney two-tailed U test. Differential LXR splicing expression  
239 levels in both TCGA BCa and Leeds TNBC tumour samples were established using  
240 multiple t-tests with Holm-Sidak for multiple correction. The knockdown siRNA  
241 experiment was analysed using a two-tailed one-way ANOVA. The relationship  
242 between protein isoform variants and their mRNA transcripts were assessed using  
243 Spearman's correlation and linear regression. ROC curves were used to establish the  
244 expression cut offs for high and low expression levels of each LXR variant. Tumour  
245 expression of each LXR variant was then assessed alongside patient survival to  
246 assess whether expression is predictive of survival in Kaplan Meier graphs. Patient  
247 survival was analysed using log-rank test.



## 248 3. Results

### 249 3.1 Database analysis of LXR transcript splice variance in breast cancer

250 To evaluate the variety of LXR splice variants, the NCBI and ENSEMBL databases  
251 were mined for mRNA transcript variants and UNIPROT database for protein variants.  
252 In total, this analysis indicated there were 64 LXR $\alpha$  transcript variants, of which 48  
253 could code for 26 LXR $\alpha$  protein variants. We found 11 LXR $\beta$  transcript variants that  
254 could code for 9 LXR $\beta$  proteins (**SF1**). These included all nine variants ( $\alpha$ 1- $\alpha$ 5,  $\beta$ 1- $\beta$ 4)  
255 later observed in breast cancer cells and/or breast tumour tissue (summarised in  
256 **Fig1**).

257 To investigate the expression of LXR splice variants in BCa, we first examined RNA-  
258 seq data from 1,103 BCa tumours in the TCGA Pan-Cancer Atlas utilising the TSVdb  
259 web-interface [19]. These data showed that out of six LXR $\alpha$  and three LXR $\beta$  splice  
260 variants with RSEM reads [26], the  $\alpha$ 1.1 (median RSEM value=231.52) and  $\beta$ 1.1  
261 (median RSEM value =1158.53) variants were most highly expressed in primary BCa  
262 samples (**Fig2A**). The  $\alpha$ 3.1 (median RSEM value=115.42),  $\alpha$ 1.2 (median RSEM  
263 value=31.88) and  $\beta$ 2 (median RSEM value=21.69) transcripts were expressed at low  
264 levels. No other transcript variants were detected in this database (**Fig2A**).

265 We further examined expression of the four variants detected at highest levels in  
266 matched tumour and normal samples from ER+ and TNBC subtypes. Both  $\alpha$ 1.1 and  
267  $\alpha$ 1.2 were expressed at significantly higher levels in ER+ and TNBC tumour tissue  
268 compared to adjacent normal tissue ( $P < 0.01$  for all; **Fig2B**).  $\alpha$ 3.1 expression was lower

269 in ER+ tumour tissue than adjacent normal ( $P=0.011$ ; **Fig2B**) but there was no  
270 difference in expression of this isoform between tumour and normal tissue in TNBC  
271 disease. There was no difference in  $\beta 1.1$  expression in either ER+ or TNBC tumours  
272 relative to adjacent normal ( $P>0.05$ ; **Fig2B**). There was no difference in expression of  
273 any individual LXR variants between ER+ and TNBC tumours (**SF4**).

274 We then examined if transcript variant expression identified in TSVdb was associated  
275 with disease-free survival (DFS) in ER+ (**Fig2C**) or TNBC patients (**Fig2D**). High  $\alpha 1.2$   
276 expression was associated with shorter DFS in ER+ patients ( $p=0.029$ ), while in TNBC  
277 patients, high  $\alpha 1.1$  expression was associated with shorter DFS ( $p=0.04$ ). Neither  $\alpha 3.1$   
278 or LXR $\beta$  expression was associated with DFS. These data suggest that elevated  
279 LXR $\alpha 1$  ( $\alpha 1$ ) may be linked to poor prognosis in breast cancer patients.

### 280 3.2 LXR expression in breast cancer cell lines

281 Having established evidence for LXR splice variant expression in the TSVdb dataset,  
282 we next examined transcript expression in a panel of BCa cell lines. HEPG2 cells  
283 express relatively high levels of both LXR $\alpha$  and LXR $\beta$  [27] so were included as a  
284 positive control. Total LXR $\alpha$  and LXR $\beta$  RNA expression was determined using SYBR  
285 green primers that target the exon 9-10 junction of LXR $\alpha$  and exon 8-9 junction for  
286 LXR $\beta$ . These exons are spliced together in every previously reported variants and in  
287 all variants described in this study (**Table-S1+S2**; **SF1-A-B**) and were used to  
288 estimate the total pool of LXR transcripts and for normalisation of variant expression.

289 The claudin high TNBC cell line MDA.MB.468 had highest expression of LXR $\alpha$  of all  
290 BCa cell lines ( $P < 0.05$ ). MDA.MB.468, MDA.MB.453 and BT474 had highest LXR $\beta$   
291 (**Fig3A-B**). In all cell lines analysed, the expression of LXR $\alpha$  mRNA was significantly  
292 lower than LXR $\beta$  (all  $p < 0.05$ ; **SF5**), recapitulating the observations from the TSVdb  
293 (**Fig2A**). Across the cell lines, the transcripts measured accounted for between 91-  
294 100% of LXR $\alpha$  (exon 9-10) and 94-102% of LXR $\beta$  (exon 8-9) exon-exon boundaries  
295 (**Fig3C-D**), indicating other variants were expressed at very low levels or did not  
296 contain the exon 9-10/7-8 boundaries. Across all cell lines we detected five mRNA  
297 species ( $\alpha 1.1$ ,  $\alpha 1.3$ ,  $\alpha 2.3$ ,  $\alpha 3.1$ ,  $\alpha 5.3$ ; **Fig3C**) predicted to code for four LXR $\alpha$  protein  
298 variants ( $\alpha 1$ ,  $\alpha 2$ ,  $\alpha 3$ ,  $\alpha 5$ ), and two coding for LXR $\beta$  ( $\beta 1$ ,  $\beta 4$ ; **Fig3D**). LXR $\alpha 5$  and LXR $\beta 4$   
299 have not been reported in the literature previously.

300  $\alpha 1$  transcripts were dominant (50-80% of all LXR $\alpha$ ) in HEPG2 and TNBC cells (**Fig3C**:  
301 note black and dark grey sections corresponding to  $\alpha 1.1$  and  $\alpha 1.3$  respectively). In  
302 the ER+ cell lines  $\alpha 5$  (40-50%) and  $\alpha 3$  (30-40%) were the majority species (**Fig3C**:  
303 note light grey and white sections corresponding to  $\alpha 5.3$  and  $\alpha 3.1$  respectively).  $\alpha 2$   
304 comprised between 5-20% depending on the cell line (**Fig3C**: hatched sections).  
305 LXR $\beta 1.1$  was detected in all BCa cell lines, with a very small amount of  $\beta 4$  transcript  
306 found in HEPG2 and the ER+ cell lines only (**Fig3D**). We successfully detected over  
307 90-100% of all the LXR variants (harbouring the exon 9-10 and 7-8 junctions) present  
308 in the cell lines. From these data, we concluded that full-length  $\alpha 1$  was the dominantly  
309 expressed variant in TNBC cells, truncated  $\alpha 5$  was the dominant LXR $\alpha$  isoform in ER  
310 positive cells, and  $\beta 1$  was the dominant LXR $\beta$  transcript across all cell types.

311 We next performed immunoblotting to establish the range of protein variants present.  
312 Representative blots and densitometry analysis show bands corresponding to  
313 predicted sizes of LXR $\alpha$ 1 ( $\approx$ 50kDa) and LXR $\beta$ 1 ( $\approx$ 55kDa) were robustly and  
314 reproducibly detected in all cell lines (**Fig3E** and **Fig3F** respectively). However,  
315 optimisation of immunoblotting experimental conditions, including antibody choice,  
316 indicated multiple additional bands were present when probing for LXR $\alpha$  (**Fig3E**).  
317 These bands closely corresponded to sizes of proteins that would be coded by the  
318 transcripts identified above, namely:  $\alpha$ 1 (50 kDa),  $\alpha$ 2 (44 kDa),  $\alpha$ 3 (46 kDa), and  $\alpha$ 5  
319 (39 kDa). The cell line specific pattern of protein expression matched that of the  
320 transcript expression;  $\alpha$ 1 RNA and protein were highly expressed in HEPG2 and the  
321 TNBC cell lines while  $\alpha$ 5 was dominant in the ER+ cells (**Fig3G**). For LXR $\beta$  only a  
322 single isoform  $\beta$ 1 was present at both RNA and protein level (**Fig3H**).

323 We concluded that in TNBC cell lines full-length LXR $\alpha$ 1 is the most abundant isoform  
324 comprising 50-80% of LXR $\alpha$  protein (depending on cell line), with two  $\alpha$ 1 transcript  
325 variants accounting for 51-75% of LXR $\alpha$  transcript. LXR $\alpha$ 3, which lacks part of the AF-  
326 1 domain and has diminished response to ligand [15] was the next most abundant  
327 producing 15-30% of the protein and 8-27% of the transcript. LXR $\alpha$ 2, which is non-  
328 responsive to ligand [15], made up 8-20% of the total LXR $\alpha$  protein coded by two  
329 transcripts producing 7-12% of the LXR $\alpha$  coding RNA (see **Supplementary**  
330 **Information Section 1** for variant nomenclature). Only a small amount of LXR $\alpha$ 5 was  
331 detected in TNBC (<10% in MDA.MB.453 cells and undetected in other TNBC lines).  
332 Interestingly, this 'double-truncation' variant that lacks both the AF-1 region of  $\alpha$ 3 and

333 the LBD region of  $\alpha 2$ , was the most abundant isoform in ER+ cells at protein (35-70%)  
334 and transcript level (43-54%).

### 335 3.3 LXR splice variant expression and clinical significance in triple 336 negative breast cancer

337 To evaluate LXR variant expression and significance in clinical samples, LXR protein  
338 expression was measured in a cohort of 38 fresh-frozen TNBC tumour samples (mean  
339 follow-up of three years), which has been reported on previously [11, 12] (Table-S3).  
340 Patients were dichotomised into two groups: 'No Event' patients defined as those who  
341 were alive and disease free at the time of last reporting or had died from unrelated  
342 reasons; 'Event' patients were those who had died from their disease and/or had  
343 disease recurrence. Representative blots are shown in **Fig4A**. Event patients had  
344 significantly higher expression than No Event patients of both full-length isoforms ( $\alpha 1$ :  
345  $p < 0.0001$ ;  $\alpha 4$ :  $p = 0.001$ ; **Fig4B**). Together  $\alpha 1$  and  $\alpha 4$  comprised 70% of the total LXR $\alpha$   
346 protein in the No Event group, but this rose to 93% in the Event group (**Fig4C**). No  
347 significant difference was observed in level of  $\alpha 2$ ,  $\alpha 3$ ,  $\alpha 5$ ,  $\beta 1$ , or  $\beta 4$  protein variants  
348 between groups (**Fig4B**).

349 When patients were dichotomised using ROC analysis, high protein expression of the  
350 full-length variants were, as expected, found associated with significantly shorter  
351 disease-free survival ( $\alpha 1$ :  $p = 0.0005$ ;  $\alpha 4$ :  $p = 0.0079$ ; **Fig4D**). Interestingly, in this more  
352 nuanced analysis, high expression of  $\alpha 5$  ( $p = 0.044$ ), LXR $\beta 1$  ( $p = 0.0023$ ), and LXR $\beta 4$   
353 ( $p = 0.037$ ) was associated with significantly longer DFS (**Fig4E**). These observations

354 were replicated when dichotomising based on RNA expression (**SF6A**). Furthermore,  
355  $\alpha$ 3.1, which codes for intact LBD but harbouring a deletion in the AF1 domain, was  
356 also associated with shorter DFS ( $p=0.022$ ; **SF6A**). The  $\alpha$ 2.3 transcript, which codes  
357 for a protein with the same LBD deletion as  $\alpha$ 5 was, like  $\alpha$ 5, associated with longer  
358 DFS ( $p=0.031$ ; **SF6A**).  $\alpha$ 2 and  $\alpha$ 3 protein however were not associated with DFS  
359 (**SF6B**). We concluded that full length LXR $\alpha$  isoforms may exacerbate disease  
360 severity, whereas those lacking the full LBD or LXR $\beta$  isoforms were associated with  
361 reduced disease severity.

## 362 3.4 Validation of isoform identity

### 363 3.4.1 Bands representing LXR variants were reduced by targeted siRNA

364 To confirm if the protein bands were LXR $\alpha$  variants, we first performed siLXR $\alpha$   
365 treatments in cell lines. Using previously validated [7] siRNA duplexes (Origene  
366 trisilencers) against LXR $\alpha$  and LXR $\beta$  we found that the protein bands predicted by size  
367 to be  $\alpha$ 1,  $\alpha$ 2,  $\alpha$ 3,  $\alpha$ 5, and  $\beta$ 1 were all significantly reduced by targeted siRNA in all cell  
368 lines tested (all  $p<0.05$ ; **SF7**). Note:  $\alpha$ 4 and  $\beta$ 4 were not expressed in cell lines so  
369 could not be validated in this way. Furthermore, siLXR $\alpha$  did not reduce LXR $\beta$   
370 expression and siLXR $\beta$  did not reduce expression of any LXR $\alpha$  isoform, and, as is  
371 characteristic of LXRs [15, 28], all protein variants were localised in the nucleus (**SF8**).

### 372 3.4.2 Unique peptides representing $\alpha$ 4 and $\beta$ 1 were identified by MS S-trap

#### 373 Mass Spectrophotometry

374 As was the case for cell line analyses, confirmation of the identity of the observed  
375 protein variants in tumour tissue was important, especially having identified the  $\alpha 4$   
376 variant which has not previously been reported in the literature. As siRNA was not  
377 possible on the tumour samples, we performed S-trap [29] coupled mass spectrometry  
378 (St-MS) in cell line and tumour lysates samples selected to represent as much of the  
379 diversity in isoforms as possible (**Table1**, **Table2**, **ST5**, **ST6**). This included two  
380 tumours in duplicate, ligand treated MDA.MB.468 cells (**SF9A**), and in siCON, siLXR $\alpha$ ,  
381 siLXR $\beta$  (**SF9B**). We found 15 peptides uniquely corresponding to  $\alpha 4$  BLAST sequence  
382 alignment indicated they were high-quality hits (100% identity), including the two first  
383 exons coding for the alternative AF1 domain in this isoform (**SF9C** – boxed amino  
384 acids) supporting our prior conclusion that  $\alpha 4$  was expressed in some tumour  
385 samples. Unique peptides of  $\beta 1$  were also detectable in our tumour sample (**SF9D** –  
386 boxed amino acids). However, unique peptides corresponding to  $\alpha 1$ ,  $\alpha 2$ ,  $\alpha 3$ ,  $\alpha 5$ , or  $\beta 4$   
387 were not produced by our enzymatic cleavage and in silico analysis indicated these  
388 isoforms would not be distinguishable from each other (**Table3**). Our next approach  
389 was to perform immunoprecipitation. We found this successfully enriched each  
390 isoform (**SF9E**) but limited amounts of tumour meant bands could not be visualised for  
391 excision on coomassie gels. We concluded that  $\alpha 4$  and  $\beta 1$  were present in tumour  
392 tissue.

### 393 3.4.3 Transcript-protein correlation analysis

394 Linear correlation analysis was performed in the seven cell lines comparing  
395 expression of each transcript variant against each protein band for which it could

396 potentially code. There was a strong and significant positive correlation between  
397 transcript variants and the protein isoform for which they were predicted to code:  $\alpha 1$   
398 protein correlated with  $\alpha 1.1$  ( $R^2=0.97$ ;  $p<0.0001$ ; **SF10** top row) and  $\alpha 1.3$  ( $R^2=0.78$ ;  
399  $p=0.0084$ ; **SF10** top row).  $\beta 1$  protein correlated with  $\beta 1.1$  transcript ( $R^2=0.99$ ;  
400  $p<0.0001$ ; **SF10** bottom row). During primer design it became clear that due to  
401 complexity arising from the large number of LXR coding transcripts, several transcripts  
402 were not distinguishable from each other due to sequence homology (see  
403 **Supplementary Information Section 1 and 2**, and denoted with asterix in **Fig3C**).  
404 Specifically, indistinguishable transcripts were:  $\alpha 1.4$  and  $\alpha 2.3$ ;  $\alpha 3.1$  and  $\alpha 5.1$ ;  $\alpha 3.3$   
405 and  $\alpha 5.3$ . We tested all potential protein isoforms for correlation with the ambiguous  
406 primer pairs:  $\alpha 1.4/\alpha 2.3$  correlated with  $\alpha 2$  protein ( $p=0.0022$ ;  $R^2=0.97$ ; **SF10** row 2)  
407 but not  $\alpha 1$  protein ( $p>0.05$ );  $\alpha 3.1/\alpha 5.1$  correlated with  $\alpha 3$  protein ( $p=0.034$ ;  $R^2=0.63$ ;  
408 **SF10** row 3) but not  $\alpha 5$  protein ( $p>0.05$ );  $\alpha 3.3/\alpha 5.3$  correlated with  $\alpha 5$  protein  
409 ( $p=0.029$ ;  $R^2=0.65$ ; **SF10** row 4) but not  $\alpha 3$  protein ( $p>0.05$ ). We also designed primers  
410 against the exon 5 and 7 junction to simultaneously recognise the  $\alpha 2$  and  $\alpha 5$  variants  
411 that lack exon 6 and a portion of the LBD. These  $\alpha 2/\alpha 5$  primers detected RNA that  
412 correlated with  $\alpha 5$  protein ( $p=0.0065$ ;  $R^2=0.8$ ; **SF10** fourth row) but not with  $\alpha 2$  ( $p>0.1$ ;  
413 **SF10** second row).

414 Next, although cytoplasmic extraction was not possible in frozen tumour samples as  
415 they had lost cellular substructure in the freezing process, given the number of  
416 replicates was larger ( $n=38$ ) we considered testing for correlations a reasonable  
417 approach (**SF11**). As for cell lines, both  $\alpha 1.1$  and  $\alpha 1.3$  correlated with  $\alpha 1$  protein



418 ( $p < 0.05$  for both);  $\alpha 2.3$  correlated with  $\alpha 2$  protein ( $p = 0.036$ );  $\alpha 3.1$  correlated with  $\alpha 3$   
419 protein ( $p = 0.056$ );  $\alpha 4.1$  correlated with  $\alpha 4$  protein ( $p = 0.0037$ ; note, this variant was  
420 not detected in cell lines);  $\alpha 5.3$  ( $p = 0.039$ ) and  $\alpha 2/\alpha 5$  ( $p = 0.054$ ) correlated with  $\alpha 5$   
421 protein. For LXR $\beta$ ,  $\beta 1.1$  transcript correlated with  $\beta 1$  protein ( $p = 0.022$ ).  $\beta 3$  and  $\beta 4$  are  
422 almost identical in size (46 and 47 kDa respectively) so are indistinguishable by  
423 immunoblotting.  $\beta 4$  transcript ( $p = 0.031$ ) but not  $\beta 3$  ( $p > 0.05$ ) correlated with the band  
424 corresponding to  $\beta 3/\beta 4$  protein (**SF11** bottom row) confirming this as LXR $\beta 4$ . In  
425 combination with the siRNA in the cell line studies above and MS experiments, these  
426 correlative observations indicate five LXR $\alpha$  variants and two LXR $\beta$  variants are  
427 expressed in TNBC.

### 428 3.5 LXR splice variants are differentially correlated with expression of 429 target genes in Event and No Event patients

430 We previously reported that LXR $\alpha$  expression is positively correlated to target gene  
431 expression in ER-negative patients who had relapsed and/or died due to their disease  
432 (Event patients) but not those who survive disease free (No Event patients) [7]. Here,  
433 we tested the hypothesis that differential LXR splice variant expression between  
434 cancers may contribute to disease aetiology via their ability to control expression of  
435 gene targets. LXR splice variant expression was tested for correlations with  
436 established LXR target genes, ABCA1 and ABCB1 [7]. Expression of both full-length  
437 isoforms ( $\alpha 1$  and  $\alpha 4$ ) positively correlated with expression of both ABCA1 or ABCB1,  
438 but interestingly only in Event patients ( $p < 0.05$  for all; **Fig5**). Strikingly, expression of  
439  $\beta 1$  was inversely correlated with both ABCA1 and ABCB1 but only in No Event patients

440 (p<0.05; **Fig5**). Statistically significant correlations between  $\alpha 2$ ,  $\alpha 3$ , or  $\alpha 5$  with target  
441 genes were not observed (**SF12**). From these data we concluded that while full length  
442 LXR $\alpha$  is associated with activation of gene targets in patients who relapse or die, LXR $\beta$   
443 is associated with inhibition of the same target genes in TNBC survivors.

## 444 Discussion

445 The objective of this study was to establish the repertoire, expression levels, and  
446 pathophysiological significance of LXR splice variants in breast cancer. In TNBC we  
447 found evidence that five LXR $\alpha$  and two LXR $\beta$  splice variants are expressed at RNA  
448 and protein levels. Three of these isoforms,  $\alpha 4$ ,  $\alpha 5$ , and  $\beta 1$ , are new to the literature  
449 and do not have validated UNIPROT records. Our data demonstrate that LXR splice  
450 variants have clinical significance in TNBC; full length LXR $\alpha$  ( $\alpha 1$  and  $\alpha 4$ ) is associated  
451 with shorter DFS, while LXR $\beta$  and LXR $\alpha$  variants with truncated ligand binding  
452 domains were associated with longer DFS.

453 We provide several lines of evidence that the LBD is required for LXR $\alpha$ 's oncogenic  
454 potential. Firstly, high expression of the full-length  $\alpha 1$  was strongly associated with  
455 shorter DFS at both transcript and protein level. High expression of two other isoforms,  
456  $\alpha 3$  (transcript only) and  $\alpha 4$  (transcript and protein) were also associated with shorter  
457 DFS. Although both have disruptions to their AF1 domains, they are otherwise  
458 homologous to full length  $\alpha 1$ , including, importantly, an uninterrupted LBD.  $\alpha 5$  skips  
459 the same exons as  $\alpha 2$  and  $\alpha 3$  and has the same deletions; 60 amino acids are missing  
460 from the LBD, and 45 amino acids of the AF1 domain are missing, respectively. These

461 truncations have been shown separately to diminish ( $\alpha 3$ ) or completely abolish ( $\alpha 2$ )  
462 transcriptional activity [15]. Interestingly, high transcript expression of  $\alpha 2$  was, like  $\alpha 5$ ,  
463 linked to longer DFS. High  $\alpha 3$  transcript on the other hand, like full length  $\alpha 1$  and  $\alpha 4$   
464 was linked to shorter DFS. These observations suggest that splice variants with  
465 disrupted LBD are advantageous, but the protein can tolerate disruption or even partial  
466 deletion of the AF1 domain and still be associated with worse prognosis.  $\beta 1$  (P55055-  
467 1) and  $\beta 4$  (M0R2F9) are generated by the mutually exclusive inclusion or exclusion of  
468 exon 7, again leading to a change in the LBD. With LXR $\beta$  however, high expression  
469 of either  $\beta 1$  and  $\beta 4$  was linked to longer DFS. The cellular role of this altered LBD  
470 remains to be determined.

471 Belorusova et al. reported peptides of LXR $\alpha$  comprising the H3 and partial part of H5  
472 correlated to high ABCA1 expression [30]. In addition, the differential relationship  
473 between target genes and LXR $\alpha$  isoforms in different patient groups also points to an  
474 oncogenic role for LXR $\alpha$  and a tumour suppressor role for LXR $\beta$  in TNBC tumours.  
475 Indeed, a beneficial role for LXR $\beta$  has been reported previously. Both dendrogenin A  
476 and RGX-104 are tumour suppressors and selective LXR $\beta$  agonists [10, 31, 32].

477 To the best of our knowledge,  $\alpha 4$  (NM\_001251934; NP\_001238863; B4DXU5),  $\alpha 5$   
478 (NM\_001363595.2; NP\_001350524.1; B5MBY7), and  $\beta 4$  (M0R2F9) have not been  
479 reported in the literature before.  $\alpha 4$  has an alternative 21 amino acids in the start of  
480 the AF1 domain producing a unique peptide mass signature that was detected with  
481 MS. These data support its inclusion in UNIPROT with a Q13133 prefix. As this variant

482 has not been investigated before and we perform no functional studies herein, the  
483 significance of this partial AF1 substitution remains unknown.  $\alpha 5$  was not detected by  
484 MS but its presumed protein band (39 kDa) was lost after siLXR $\alpha$  treatment, its  
485 transcript was robustly expressed, and protein and transcript expression were strongly  
486 correlated. Although a unique peptide for  $\beta 4$  was predicted from *in silico* analyses it  
487 was not detected with MS, however, its transcript was robustly expressed, and protein  
488 and transcript expression were strongly correlated.

489 Some of our results are at odds with prior observations. We were unable to detect  
490 expression of XP\_02430405X (previously termed  $\alpha 4$  [16]), in any cell lines or tissues,  
491 at RNA or protein level, including in HEPG2 or MCF7 cell lines that were previously  
492 shown to express this isoform [16, 33]. Intriguingly, a variant previously reported to be  
493  $\alpha 5$  [16, 33] did not correspond to any of the 64 LXR $\alpha$  transcripts from NCBI, nor any  
494 LXR $\alpha$  UNIPROT entries (**SF2A**). In this study [16], the measurement of  
495 XP\_02430405X and previously reported  $\alpha 5$  relied on PCR primers that detected a  
496 retained intron between exon 6-7 and a retained intron between exon 7-8, respectively  
497 (**SF2A**). We went to extensive lengths to ensure primary RNA or gDNA did not  
498 contaminate our cDNA libraries, steps that surprisingly have not been reported in LXR  
499 splicing studies previously. Cytoplasmic RNA is preferred over total cell isolates when  
500 examining splice expression and this has been reported previously to increase  
501 sensitivity of splice junction detection [34]. Previous detection of XP\_02430405X may  
502 therefore be due to amplification of incompletely processed transcripts or  
503 contaminating gDNA. During our primer design stage, we found that the PCR primers

504 previously used to measure  $\alpha 1$  at the exon 2-3 junction [15, 16, 35] also detect  $\alpha 2$   
505 **(SF3)**. In addition, primers previously used to measure  $\alpha 2$  at the exon 5-7 junction [15,  
506 16, 35] also detect the previously unreported  $\alpha 5$  variant **(SF2)**. Our correlation  
507 analyses in cell lines and primary tumour samples suggest the majority of exon 6  
508 skipping transcripts actually code for  $\alpha 5$  not  $\alpha 2$ . We also found  $\alpha 5$  is significantly (20-  
509 fold) higher than  $\alpha 2$  in MCF7 and equal to  $\alpha 2$  in HEPG2, the same cell lines that in  
510 prior studies were used to show  $\alpha 2$  was strongly expressed. It likely that previous  
511 reports have over-estimated the contribution of  $\alpha 2$  and under-estimated the  
512 contribution of  $\alpha 5$  to the LXR pool.

513 In summary, this study provides critical insight into the pathophysiology of LXR splicing  
514 in BCa. Our study clarifies the relative roles of the LXR $\alpha$  and LXR $\beta$  isoforms and our  
515 data are consistent with the hypothesis that while full length LXR $\alpha$  is oncogenic, LXR $\beta$   
516 and truncated LXR $\alpha$  variant ( $\alpha 5$ ) can act as tumour suppressors. We propose the  
517 existence of two new LXR $\alpha$  isoforms:  $\alpha 4$  containing an alternative AF1 region, and  $\alpha 5$   
518 which lacks large sections of the AF1 and LBD, probably rendering it with dominant  
519 negative function.

520 Triple negative breast cancer is defined as a category of exclusion. The data  
521 presented here suggest that measuring LXR $\alpha 1$ , LXR $\alpha 5$ , and LXR $\beta$  at RNA or protein  
522 level may allow sub-stratification of TNBC patients for increased accuracy of  
523 prognosis. Perhaps more importantly, given the array of pharmacological and dietary  
524 modulators of the LXR pathway, defining gene networks regulated by the opposing

525 oncogenic and tumour suppressor LXR variants will aid in the development of lifestyle  
526 and pharmacological interventions to reduce incidence and improve survival in this  
527 challenging cancer of unmet clinical need.

## 528 Figure Legends

529 Figure 1. Schematic diagram of (A) LXR $\alpha$  and (B) LXR $\beta$  splice variants detected at  
530 RNA and protein level in this study. AF1=Activation Function 1; DBD=DNA Binding  
531 Domain; H=hinge; LBD=Ligand Binding Domain. The numbers right below the isoform  
532 domain boxes are represented the position of amino acids.

533 Figure 2. LXR Splicing events in BCa validated by TCGA Splicing Variants database  
534 (TSVdb). (A) Heatmap visualization of normalized RSEM (RNA-Seq by Expectation  
535 Maximization) value expression of LXR $\alpha$  and LXR $\beta$  in 1,103 TCGA BCa samples.  
536 Note: Transcript uc002prv was only reported in TSVdb and is not recorded in NCBI,  
537 ENSEMBL, or UNIPROT databases. (B) Comparison of LXR transcript variant  
538 expression, for  $\alpha$ 1.1,  $\alpha$ 1.2,  $\alpha$ 3.1, and  $\beta$ 1.1, in matched tumour and normal tissues  
539 grouped by BCa subtype, ER+ (n=78) and TNBC (n=18). Statistical analysis by Man-  
540 Whitney two tailed U tests.  $P \leq 0.05$  was considered significant. (C, D) Kaplan-Meier  
541 survival curves plotting disease free survival of TCGA BCa patients. The TCGA BCa  
542 samples (downloaded from TSVdb TCGA splicing database) were grouped by BCa  
543 subtype, (C) ER+ (n=803) and (D) TNBC (n=101). Survival curves of each subtype  
544 were separated into two groups, no event (ER+=675, TNBC=79) and event (ER+=128;

545 TNBC=22) based on their overall survival data reported in cBioportal. P-value is based  
546 on the log-rank test and data groups were considered significantly different if  $p < 0.05$ .

547 Figure 3. Diversity of LXR splice variants in breast cancer cell line panel. RNA  
548 analyses of total LXR $\alpha$  (A) and LXR $\beta$  (B) expression. The stacked bar graphs show  
549 LXR $\alpha$  (C) and LXR $\beta$  (D) transcript variants normalised to ubiquitously expressed exon-  
550 exon junctions. Asterix denote ambiguous amplicons. Representative blots and  
551 densitometry of LXR $\alpha$  (E) and LXR $\beta$  (F) protein variants observed in cell lines. Pie  
552 charts show contribution of each transcript variant and protein variant to the total  
553 amount of LXR $\alpha$  (G) and LXR $\beta$  (H). All data shown are mean of three independent  
554 replicates with SEM. Statistical significance was measured by two-tailed one-way  
555 ANOVA and significant differences are denoted with different letters if  $p \leq 0.05$ .

556 Figure 4. LXR $\alpha$ 1 and LXR $\alpha$ 4 are highly expressed in TNBC patients with poor survival.  
557 Representative blots showing the LXR splicing events in tumours derived from 38  
558 TNBC patients, who were either free from disease (no event;  $n=23$ ) or who had  
559 relapsed or died (event;  $n=15$ ) after follow-up (A). Differential expression of LXR $\alpha$  and  
560 LXR $\beta$  protein variants in No Event and Event groups were plotted in box and whiskers  
561 charts (B). The line shows the median value, the box shows 10th to 90th percentile  
562 and whiskers show minimum to maximum values. Statistical analysis was established  
563 using multiple *t*-tests with Holm-Sidak for multiple correction,  $p \leq 0.05$  was considered  
564 significant. Pie charts show contribution of each transcript variant and protein variant  
565 to the total amount of LXR $\alpha$  in No Event and Event patients (C). Kaplan-Meier survival  
566 curves plotting disease free survival of TNBC patients dichotomised based on protein

567 expression of full length LXR $\alpha$ 1 and LXR $\alpha$ 4 transcripts (D), or truncated LXR $\alpha$ 5 and  
568 LXR $\beta$ 1 and LXR $\beta$ 4 (E). All protein measured relative to HPRT. Data derived from the  
569 mean of two different slices of tumours. Significance determined by the Log-rank  
570 (Mantel-cox) test where  $p \leq 0.05$  was considered significant.

571 Figure 5. Protein expression of LXR variants is differentially associated with LXR target  
572 gene expression in TNBC tumours. TNBC patients (n=38) were divided into two  
573 groups, no event (n=23) and event (n=15) based on disease-free survival status.  
574 Linear regression was used to determine if the slope of the lines were significantly  
575 different from 0 ( $p \leq 0.05$ ). Line of best fit are shown if the relationship was significant.  
576 Circles represent mean protein expression of two tumour slices for individual TNBC  
577 patients.

## 578 Acknowledgments

579 The mass spectrometry was performed and analysis supported by Dr James Ault and  
580 Dr Rachel George at the Biomolecular Mass Spectrometry Facility, Faculty of  
581 Biological Sciences, University of Leeds.

## 582 Funding Statement

583 Ms Priscilia Lianto was jointly funded by a Leeds International Doctoral Scholarship  
584 and the University of Leeds School of Food Science and Nutrition.

## 585 References



- 586 [1] F. Bray, J. Ferlay, I. Soerjomataram, R.L. Siegel, L.A. Torre, A. Jemal, Global cancer  
587 statistics 2018: GLOBOCAN estimates of incidence and mortality worldwide for 36 cancers  
588 in 185 countries, *CA: a cancer journal for clinicians* 68(6) (2018) 394-424.
- 589 [2] C.A. Hudis, L. Gianni, Triple-negative breast cancer: an unmet medical need, *Oncologist*  
590 16 (2011).
- 591 [3] WCRF/AICR, Continuous Update Project Report: Diet, Nutrition, Physical Activity and  
592 Cancer, World Cancer Research Fund International/American Institute for Cancer Research  
593 2017.
- 594 [4] B. Liu, Z. Yi, X. Guan, Y.X. Zeng, F. Ma, The relationship between statins and breast  
595 cancer prognosis varies by statin type and exposure time: a meta-analysis, *Breast Cancer Res*  
596 *Treat* 164(1) (2017) 1-11.
- 597 [5] L. Jiang, X. Zhao, J. Xu, C. Li, Y. Yu, W. Wang, L. Zhu, The Protective Effect of Dietary  
598 Phytosterols on Cancer Risk: A Systematic Meta-Analysis, *Journal of Oncology* 2019 (2019)  
599 11.
- 600 [6] G. Cioccoloni, C. Soteriou, A. Websdale, L. Wallis, M.A. Zulyniak, J.L. Thorne,  
601 Phytosterols and phytostanols and the hallmarks of cancer in model organisms: A systematic  
602 review and meta-analysis, *Crit Rev Food Sci Nutr* (2020) 1-21.
- 603 [7] S.A. Hutchinson, A. Websdale, G. Cioccoloni, H. Roberg-Larsen, P. Lianto, B. Kim, A.  
604 Rose, C. Soteriou, A. Pramanik, L.M. Wastall, B.J. Williams, M.A. Henn, J.J. Chen, L. Ma,  
605 J.B. Moore, E. Nelson, T.A. Hughes, J.L. Thorne, Liver x receptor alpha drives  
606 chemoresistance in response to side-chain hydroxycholesterols in triple negative breast cancer,  
607 *Oncogene* (2021).
- 608 [8] E.R. Nelson, S.E. Wardell, J.S. Jasper, S. Park, S. Suchindran, M.K. Howe, N.J. Carver,  
609 R.V. Pillai, P.M. Sullivan, V. Sondhi, 27-Hydroxycholesterol links hypercholesterolemia and  
610 breast cancer pathophysiology, *Science* 342(6162) (2013) 1094-1098.
- 611 [9] A.E. Baek, A.Y. Yen-Rei, S. He, S.E. Wardell, C.-Y. Chang, S. Kwon, R.V. Pillai, H.B.  
612 McDowell, J.W. Thompson, L.G. Dubois, The cholesterol metabolite 27 hydroxycholesterol  
613 facilitates breast cancer metastasis through its actions on immune cells, *Nature*  
614 *communications* 8(1) (2017) 1-11.
- 615 [10] M. Poirot, S. Silvente-Poirot, The tumor-suppressor cholesterol metabolite, dendrogenin  
616 A, is a new class of LXR modulator activating lethal autophagy in cancers, *Biochem Pharmacol*  
617 153 (2018) 75-81.
- 618 [11] S.A. Hutchinson, P. Lianto, H. Roberg-Larsen, S. Battaglia, T.A. Hughes, J.L. Thorne,  
619 ER-Negative Breast Cancer Is Highly Responsive to Cholesterol Metabolite Signalling,  
620 *Nutrients* 11(11) (2019) 2618.
- 621 [12] S. Solheim, S.A. Hutchinson, E. Lundanes, S.R. Wilson, J.L. Thorne, H. Roberg-Larsen,  
622 Fast liquid chromatography-mass spectrometry reveals side chain oxysterol heterogeneity in  
623 breast cancer tumour samples, *The Journal of steroid biochemistry and molecular biology* 192  
624 (2019) 105309.
- 625 [13] P.J. Willy, K. Umesono, E.S. Ong, R.M. Evans, R.A. Heyman, D.J. Mangelsdorf, LXR, a  
626 nuclear receptor that defines a distinct retinoid response pathway, *Genes & development* 9(9)  
627 (1995) 1033-1045.
- 628 [14] D.M. Shinar, N. Endo, S.J. Rutledge, R. Vogel, G.A. Rodan, A. Schmidt, NER, a new  
629 member of the gene family encoding the human steroid hormone nuclear receptor, *Gene* 147(2)  
630 (1994) 273-276.

- 631 [15] M. Chen, S. Beaven, P. Tontonoz, Identification and characterization of two alternatively  
632 spliced transcript variants of human liver X receptor alpha, *J Lipid Res* 46(12) (2005) 2570-9.
- 633 [16] K. Endo-Umeda, S. Uno, K. Fujimori, Y. Naito, K. Saito, K. Yamagishi, Y. Jeong, H.  
634 Miyachi, H. Tokiwa, S. Yamada, M. Makishima, Differential expression and function of  
635 alternative splicing variants of human liver X receptor alpha, *Mol Pharmacol* 81(6) (2012) 800-  
636 10.
- 637 [17] K. Hashimoto, E. Ishida, S. Matsumoto, N. Shibusawa, S. Okada, T. Monden, T. Satoh,  
638 M. Yamada, M. Mori, A liver X receptor (LXR)- $\beta$  alternative splicing variant (LXRBSV) acts  
639 as an RNA co-activator of LXR- $\beta$ , *Biochemical and biophysical research communications*  
640 390(4) (2009) 1260-1265.
- 641 [18] A.J. Annalora, C.B. Marcus, P.L. Iversen, Alternative Splicing in the Nuclear Receptor  
642 Superfamily Expands Gene Function to Refine Endo-Xenobiotic Metabolism, *Drug Metab*  
643 *Dispos* 48(4) (2020) 272-287.
- 644 [19] W. Sun, T. Duan, P. Ye, K. Chen, G. Zhang, M. Lai, H. Zhang, TSVdb: a web-tool for  
645 TCGA splicing variants analysis, *BMC genomics* 19(1) (2018) 405.
- 646 [20] E. Cerami, J. Gao, U. Dogrusoz, B.E. Gross, S.O. Sumer, B.A. Aksoy, A. Jacobsen, C.J.  
647 Byrne, M.L. Heuer, E. Larsson, The cBio cancer genomics portal: an open platform for  
648 exploring multidimensional cancer genomics data, *AACR*, 2012.
- 649 [21] R.V. Broad, S.J. Jones, M.C. Teske, L.M. Wastall, A.M. Hanby, J.L. Thorne, T.A.  
650 Hughes, Inhibition of interferon-signalling halts cancer-associated fibroblast-dependent  
651 protection of breast cancer cells from chemotherapy, *British Journal of Cancer* 124(6) (2021)  
652 1110-1120.
- 653 [22] J.L. Thorne, S. Battaglia, D.E. Baxter, J.L. Hayes, S.A. Hutchinson, S. Jana, R.A.  
654 Millican-Slater, L. Smith, M.C. Teske, L.M. Wastall, T.A. Hughes, MiR-19b non-canonical  
655 binding is directed by HuR and confers chemosensitivity through regulation of P-glycoprotein  
656 in breast cancer, *Biochimica et Biophysica Acta (BBA) - Gene Regulatory Mechanisms*  
657 (2018).
- 658 [23] A. Untergasser, I. Cutcutache, T. Koressaar, J. Ye, B.C. Faircloth, M. Remm, S.G. Rozen,  
659 Primer3—new capabilities and interfaces, *Nucleic acids research* 40(15) (2012) e115-e115.
- 660 [24] K. Suzuki, P. Bose, R.Y. Leong-Quong, D.J. Fujita, K. Riabowol, REAP: A two minute  
661 cell fractionation method, *BMC research notes* 3(1) (2010) 294.
- 662 [25] E. Gasteiger, C. Hoogland, A. Gattiker, S. Duvaud, M. Wilkins, R. Appel, A. Bairoch,  
663 *The Proteomics Protocols Handbook: Protein Identification and Analysis Tools on the ExPASy*  
664 *Server*, Humana Press, 2003.
- 665 [26] B. Li, C.N. Dewey, RSEM: accurate transcript quantification from RNA-Seq data with or  
666 without a reference genome, *BMC bioinformatics* 12(1) (2011) 1-16.
- 667 [27] B.A. Laffitte, S.B. Joseph, R. Walczak, L. Pei, D.C. Wilpitz, J.L. Collins, P. Tontonoz,  
668 Autoregulation of the human liver X receptor  $\alpha$  promoter, *Molecular and cellular biology*  
669 21(22) (2001) 7558-7568.
- 670 [28] K. Prüfer, J. Boudreaux, Nuclear localization of liver X receptor  $\alpha$  and  $\beta$  is differentially  
671 regulated, *Journal of cellular biochemistry* 100(1) (2007) 69-85.
- 672 [29] K. Hayoun, D. Gouveia, L. Grenga, O. Pible, J. Armengaud, Evaluation of sample  
673 preparation methods for fast proteotyping of microorganisms by tandem mass spectrometry,  
674 *Frontiers in microbiology* 10 (2019) 1985.

- 675 [30] A.Y. Belorusova, E. Evertsson, D. Hovdal, J. Sandmark, E. Bratt, I. Maxvall, I.G.  
676 Schulman, P. Åkerblad, E.-L. Lindstedt, Structural analysis identifies an escape route from the  
677 adverse lipogenic effects of liver X receptor ligands, *Communications biology* 2(1) (2019) 1-  
678 13.
- 679 [31] G. Segala, M. David, P. de Medina, M.C. Poirot, N. Serhan, F. Vergez, A. Mougel, E.  
680 Saland, K. Carayon, J. Leignadier, Dendrogenin A drives LXR to trigger lethal autophagy in  
681 cancers, *Nature communications* 8(1) (2017) 1-17.
- 682 [32] M.F. Tavazoie, I. Pollack, R. Tanquedo, B.N. Ostendorf, B.S. Reis, F.C. Gonsalves, I.  
683 Kurth, C. Andreu-Agullo, M.L. Derbyshire, J. Posada, S. Takeda, K.N. Tafreshian, E.  
684 Rowinsky, M. Szarek, R.J. Waltzman, E.A. McMillan, C. Zhao, M. Mita, A. Mita, B.  
685 Chmielowski, M.A. Postow, A. Ribas, D. Mucida, S.F. Tavazoie, LXR/ApoE Activation  
686 Restricts Innate Immune Suppression in Cancer, *Cell* 172(4) (2018) 825-840.e18.
- 687 [33] J. Bunay, A. Fouache, A. Trousson, C. de Joussineau, E. Bouchareb, Z. Zhekun, A. Kocer,  
688 L. Morel, S. Baron, J.-M.A. Lobaccaro, Screening for Liver X Receptor modulators: where are  
689 we and for what use?, *British Journal of Pharmacology* (2020).
- 690 [34] A. Zaghlool, A. Ameer, L. Nyberg, J. Halvardson, M. Grabherr, L. Cavelier, L. Feuk,  
691 Efficient cellular fractionation improves RNA sequencing analysis of mature and nascent  
692 transcripts from human tissues, *BMC biotechnology* 13(1) (2013) 99.
- 693 [35] C. Rondanino, L. Ouchchane, C. Chauffour, G. Marceau, P. Dechelotte, B. Sion, H. Pons-  
694 Rejraji, L. Janny, D.H. Volle, J.M. Lobaccaro, F. Brugnon, Levels of liver X receptors in  
695 testicular biopsies of patients with azoospermia, *Fertil Steril* 102(2) (2014) 361-371 e5.

Table 1. LXR $\alpha$  peptides detected by S-trap column coupled with Mass Spectrometry (MS). Amino acids position numbers based on LXR $\alpha$ 1 structure. The grey highlight indicated unique peptides of LXR variant detected by MS.

Sample	Total identified peptides		-10lgP [LXR $\alpha$ ]	Coverage LXR $\alpha$ peptides	Supporting peptides [LXR $\alpha$ ]	Unique	Amino acids position	
							start	end
Tumour 2 rep 1	3500	52.32	13%	Q.AQ(+.98)GGSSC(+57.02)ILR.E	No	32	41	
				A.QGGSSC(+57.02)ILR.E	No	33	41	
				R.MPHSAGGTAGV.G	No	46	56	
				R.ASSPPQ(+.98)ILPQ.L	No	196	205	
				R.ASSPPQILPQLSPEQ(+.98)LGMIEK.L	No	196	216	
				R.AMN(+.98)ELQLN(+.98)DAEFALLI.A	No	345	360	
Tumour 2 Rep 2	3971	58.66	22%	K.C(+57.02)RQ(+.98)AGM(+15.99)REEC(+57.02)VLSEEQ(+.98)IRLK.K	No	158	177	
				R.QEEEQAHATSLPPR.A	No	182	195	
				R.ASSPPQILPQLSPEQ(+.98)LGMIEK.L	No	196	216	
				L.SPEQ(+.98)LGMIEK.L	No	207	216	
				G.M(+15.99)IEKLVAQQ(+.98)Q(+.98).C	No	213	223	
				K.QLPGFLQLSR.E	No	274	283	
				Q.VEFINPIFEFSR.A	No	333	344	
				R.AMNELQLNDAEFALLI.A	No	345	360	
Tumour 5 Rep 1	3713	61.52 [ $\alpha$ 4 +LXR $\alpha$ homolog]	19%	MQ(+.98)QTSWN(+.98)PLGGTC(+57.02)K.Q	Yes [ $\alpha$ 4]	-14	-1	
		59.30 [LXR $\alpha$ homolog]	16%	R.AEPPSEPTAIRPQ(+.98)K.R	No	70	83	
				KC (+57.02)RQAGMR.E	No	196	208	
				R.ASSPPQILPQLSP.E	No	196	208	
				R.ASSPPQILPQLSPEQ(+.98)LGMIEK.L	No	196	216	
				G.MIEKLVAQQQC(+57.02)NRR.S	No	213	227	
				K.TSAIEVMLLETSTRRYN(+.98)PG.S	No	292	309	

Tumour 5 Rep 2	3412	38.73	9%	C.VLSEEQIR.L	No	168	175
				R.ASSPPQILPQLSPEQ(+.98)LGMIEK.L	No	196	216
				R.ASSPPQ(+.98)ILPQ.L	No	196	205
				R.EDQIALLK.T	No	284	291

Table 2. LXR $\beta$  peptides detected by S-trap column coupled with Mass Spectrometry (MS). Amino acids position numbers based on LXR $\beta$ 1 structure. The grey highlight indicated unique peptides of LXR variant detected by MS.

Sample	Total identified peptides	-10lgP [LXR $\beta$ ]	Coverage LXR $\beta$ peptides	Supporting peptides [LXR $\beta$ ]	Unique	Amino acids position	
						start	end
Tumour 2 Rep 1	3500	46.60	7%	L.MIQQLVAAQ.L	No	226	234
				Q.Q(+.98)LVAAQLQC(+57.02)NK.R	No	229	239
				Q.VEFINPIFEFSR.A	No	346	357
				K.RPQDQ(+.98)LR.F	No	410	416
Tumour 2 rep 2	3971	39.62	10%	R.RSVRGGAR.R	No	113	121
				K.EAGM(+15.99)REQ(+.98)C(+57.02)VLSEEQIRKK.K	No	151	168
				K.VTPWPLGADPQSR.D	Yes [ $\beta$ 1]	248	260
				K.RPQDQ(+.98)LR.F	No	410	416
Tumour 5 Rep 1	3713	56.33	14%	R.SVVRGGAR.R	No	113	121
				E.LM(+15.99)IQQ(+.98)LVAAQ.L	No	225	234
				V.QLTAAQ(+.98)ELMIQ(+.98).Q	No	218	228
				Q.Q(+.98)LVAAQLQC(+57.02)NK.R	No	229	239
				K.RSFSDQ(+.98)PK.V	No	240	247
				K.VTPWPLGADPQ(+.98)SR.D	Yes [ $\beta$ 1]	248	260
				A.LQQ(+.98)PYVEALLS.Y	No	394	404
E.ALLSYTR.I	No	401	407				
Tumour 5 Rep 2	3412	59.82	20%	R.RSVRGGAR.R	No	113	121
				C.VLSEEQIR.K	No	159	166
				R.KQ(+.98)QQ(+.98)ESQSQSQSPVGPQG.S	No	172	189

E.GVQLTAAQ(+.98)ELMIQ.Q	No	216	228
E.LM(+15.99)IQQ(+.98)LVAAQ.L	No	225	234
Q.QLVAAQ(+.98)LQ(+.98)C(+57.02)N(+.98)K.R	No	229	239
K.RSFSDQ(+.98)PK.V	No	240	247
R.EDQIALLK.A	No	297	304
A.LQQ(+.98)PYVEALLS.Y	No	394	404
K.RPQDQ(+.98)LR.F	No	410	416

Table 3. Unique peptides of LXR variants. Amino acids position number based on  $\alpha 1$  and/or  $\beta 1$  amino acid numbering position. Amino acid numbering position with “-“ indicates the additional amino acid(s) coming before  $\alpha 1$  and/or  $\beta 1$ 's amino acid position number 1. The numerical exons represent the first-discovered exons. The numerical exons followed with alphabets represent the later-discovered exons.

LXR	Also, recognise	Peptide mass	Amino acid position (based on LXRa1 structure)		Exon	Unique peptides (after trypsin digestion)
			start	end		
$\alpha 1$	$\alpha 2$	1607.8137	1	15	2	MSLWLGAPVPDIPPD
		1348.7140	293	300	6	SAIEVMLETSR
$\alpha 2$	$\alpha 5$	1148.6343	235,236-297	300	5/7	VT-VMLETSR
$\alpha 3$	$\alpha 5$	2307.1761	46	69	3	MPHSAGGTAGVGLEAAEPTALLTR
$\alpha 4$	-	1550.7090	-14	-1	-1d	MQQTSWNPLGGTCK
		554.3045	-19	-15	-1d	QPPGR

XP_0243040XXX -	2942.3842 1170.5538 1005.4669 741.3890 590.3079 510.2381	Additional 64 amino acids due to the presence of a retained intron in between exon 6 and 7		Exon -7a	GEAEDWYLDWEGPPDIELGEP NLLGSR DEENRPPWK EVAGEGQGMK TSPSPR RPCSK FAACV
$\beta$ 1	1423.7328 1475.7892	248 268	260 279	Exon6/ exon7abc	<u>VTPWPLGADPQSR</u> <u>FAHFTELAISVQ</u>
$\beta$ 3	1021.5564	249-280	286	Exon6/ exon7b	<u>V-TEIVDFAK</u>
$\beta$ 4	545.3405	249-293	299	Exon6/ Exon 7c	<u>V-TLGREDQ</u>





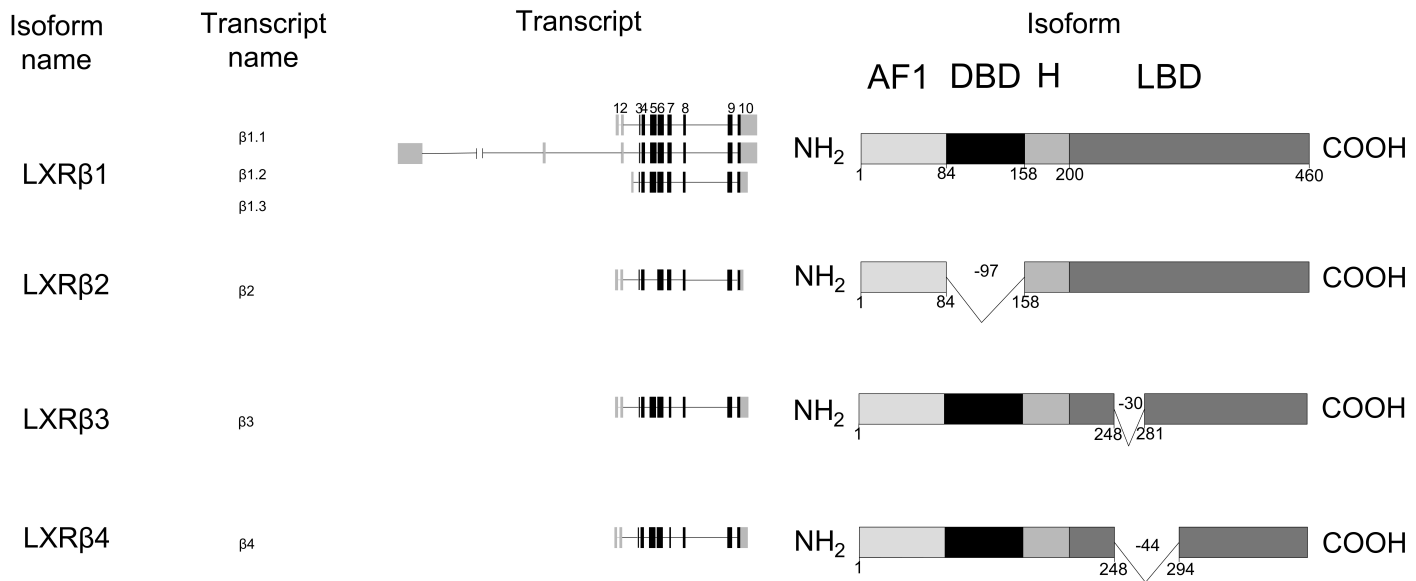
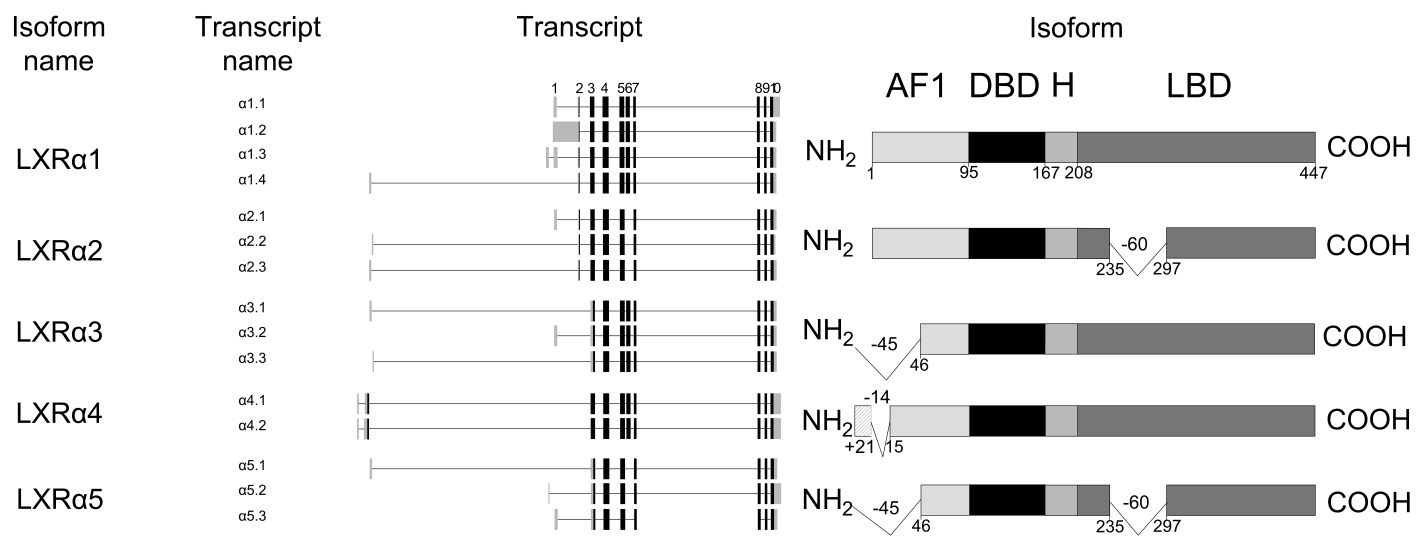


Figure 1

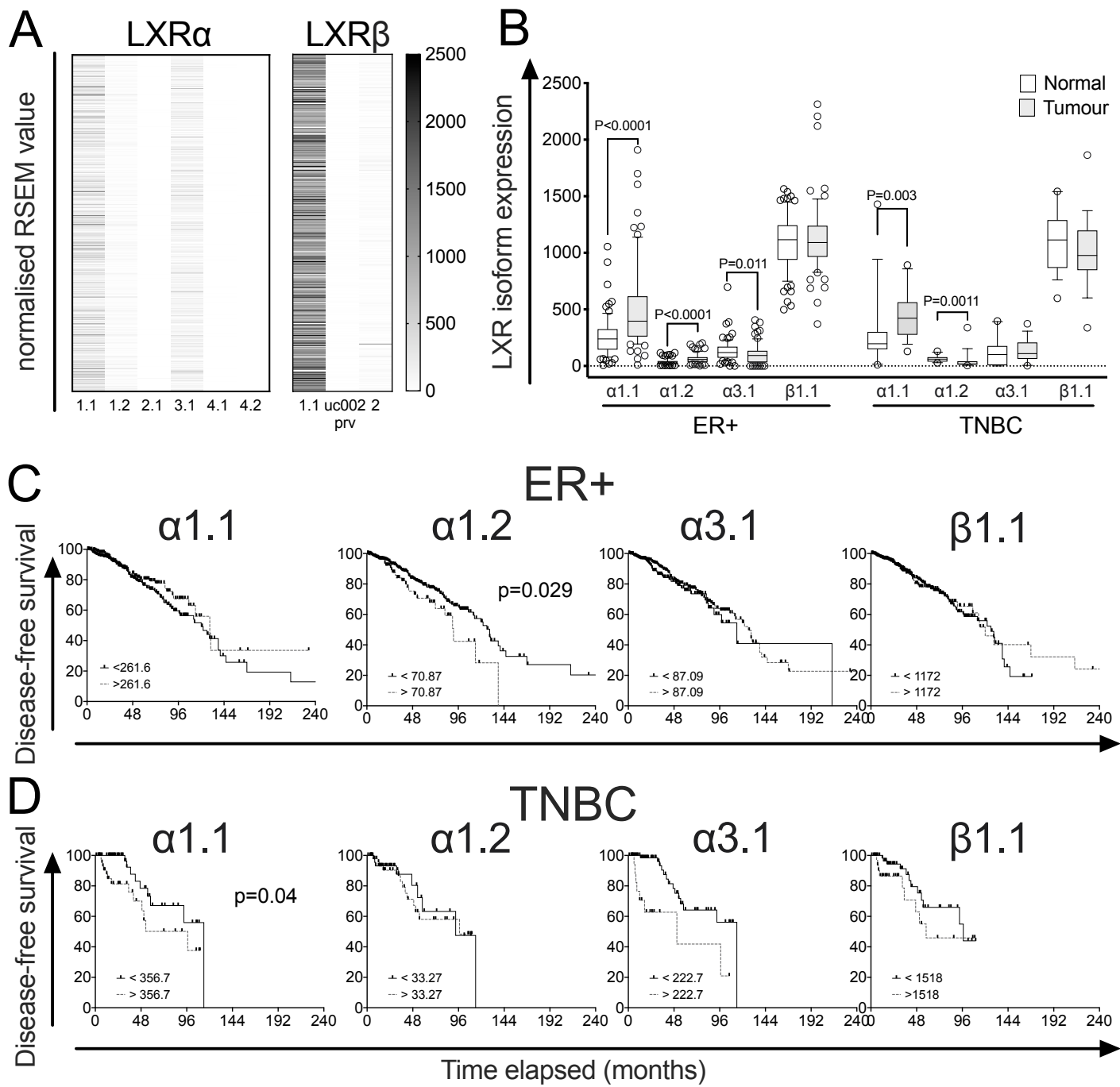
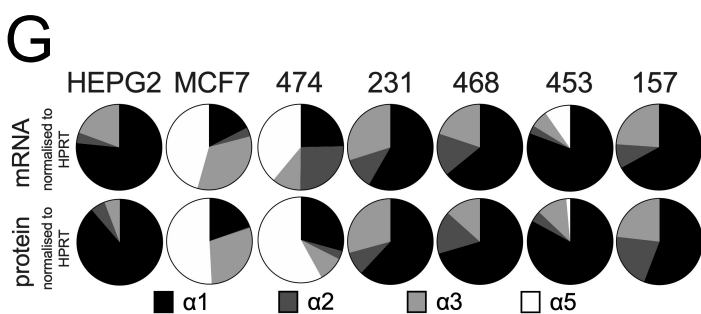
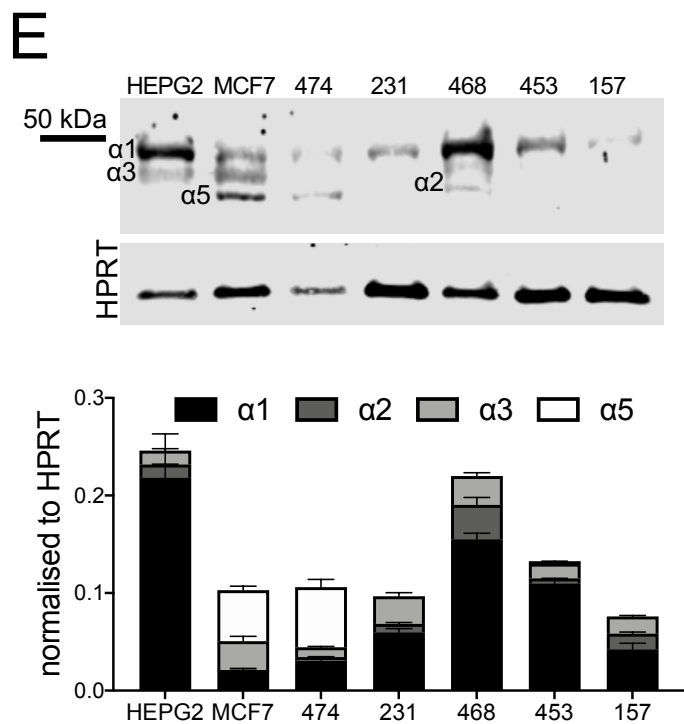
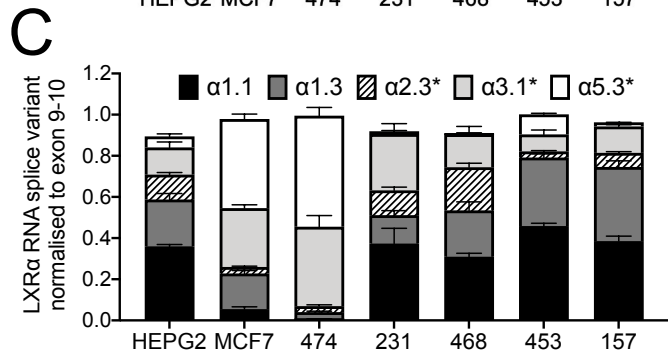
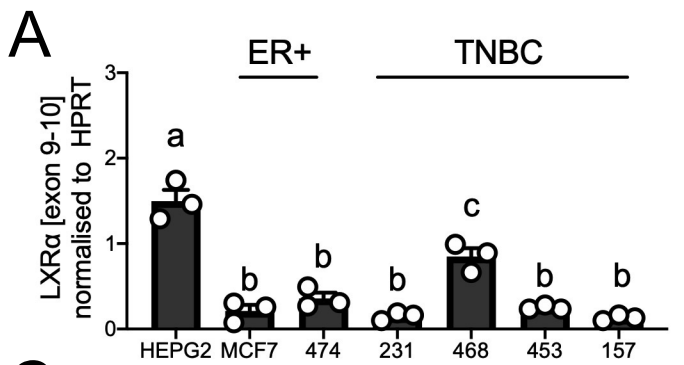
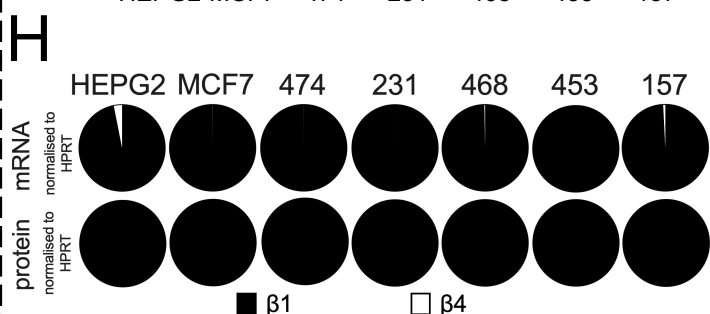
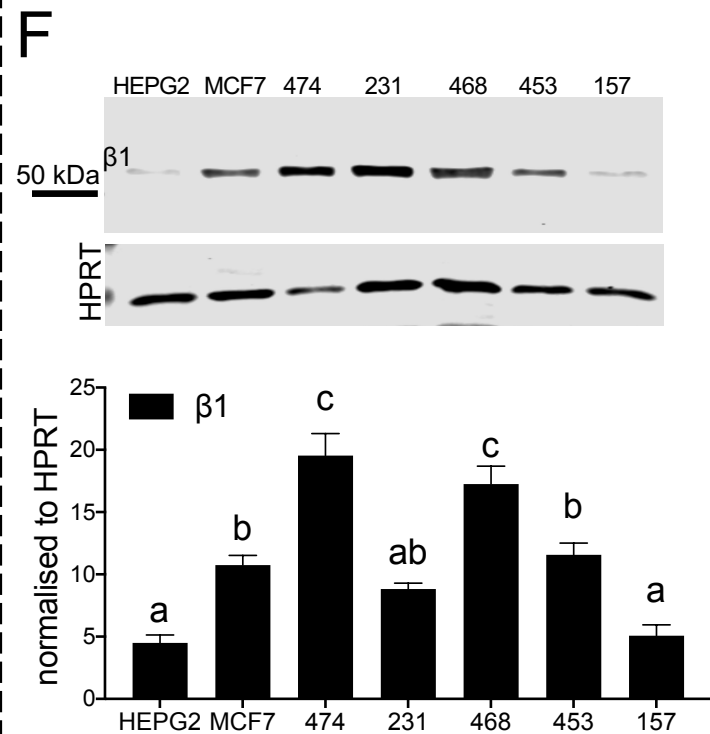
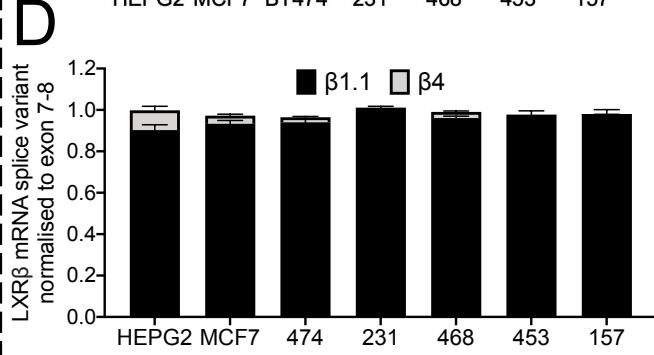
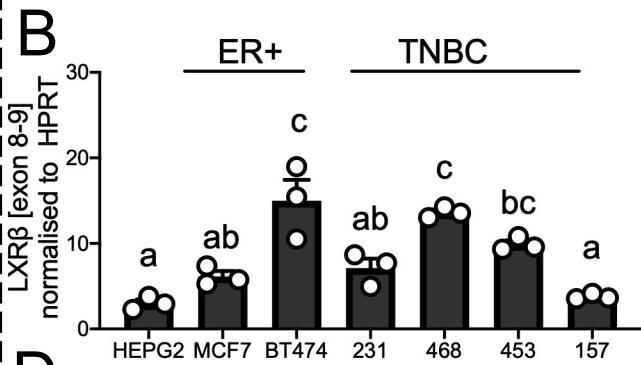


Figure 2

# LXR $\alpha$



# LXR $\beta$



**Figure 3**

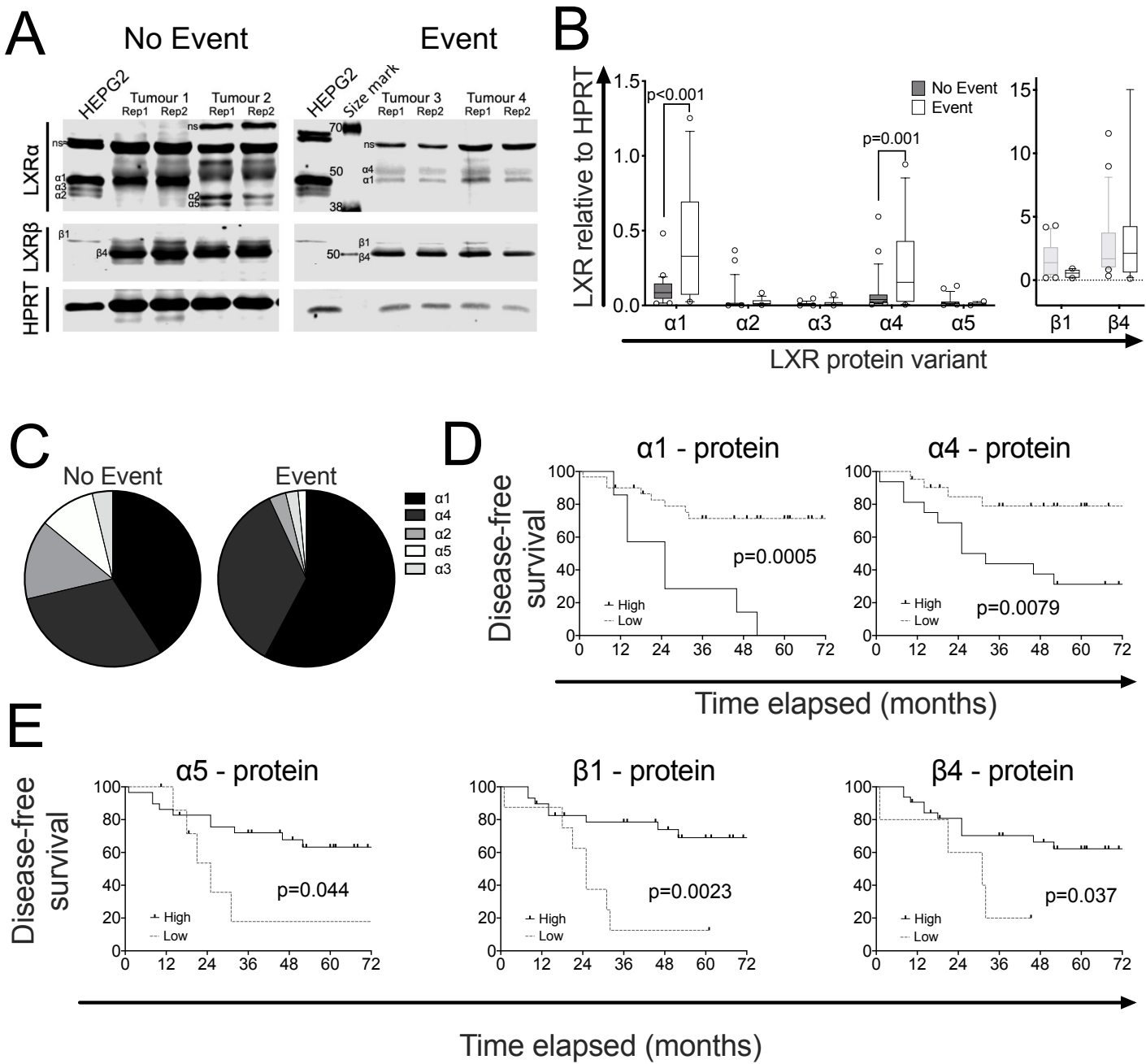


Figure 4

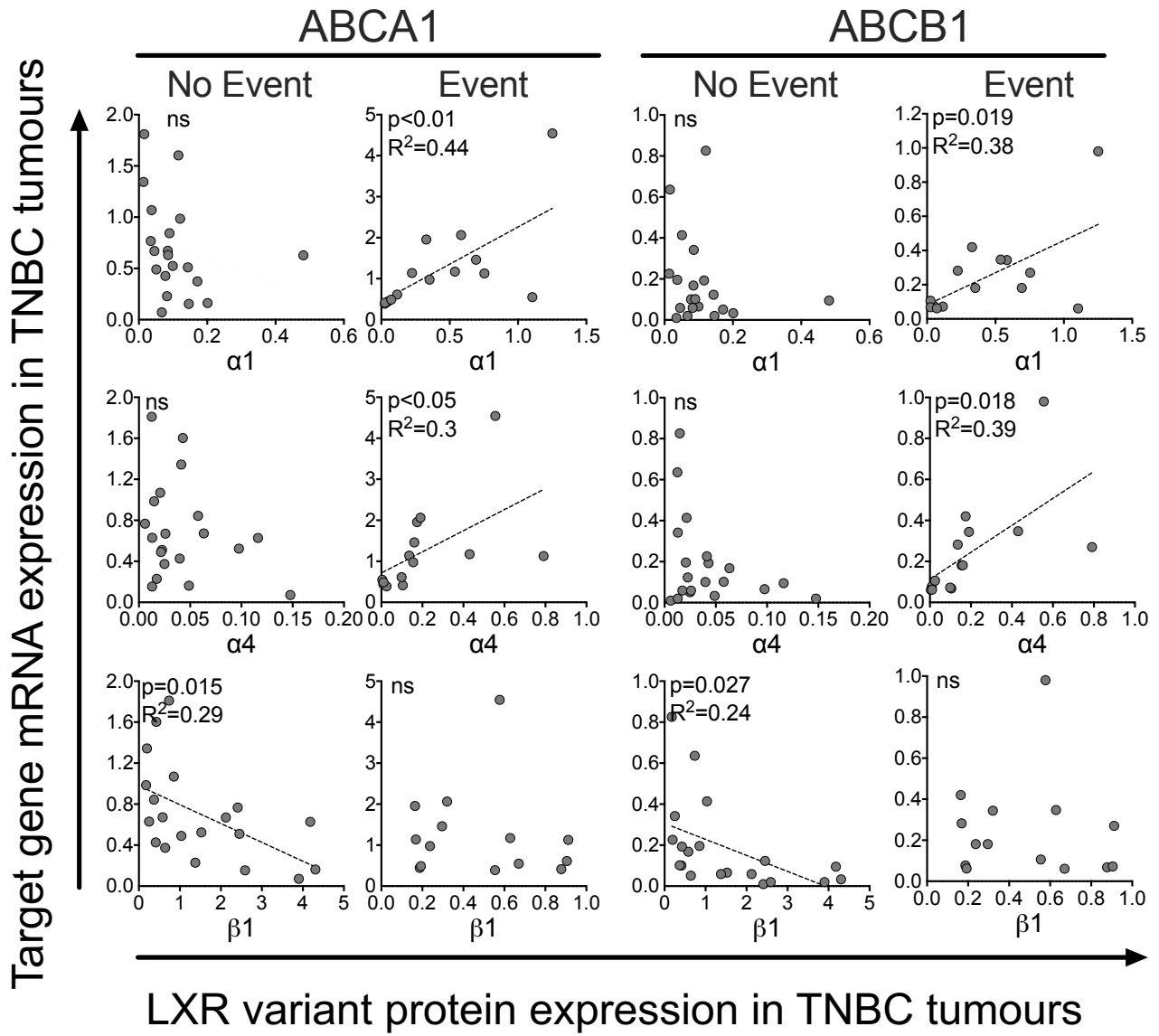


Figure 5